

### Standards for Performance Measurements in Scintillation Cameras

Gerd Muehlelehner,\* Robert H. Wake, and Richard Sano

*Siemens Gammasonics, Des Plaines, Illinois, Technicare, Solon, Ohio, and Picker Corporation, Cleveland, Ohio*

**Performance measurements of scintillation cameras are made (a) by the manufacturer to test and specify the equipment he sells, (b) by the customer as part of his acceptance testing, and (c) by the user as part of a periodic quality-control program. This paper describes the NEMA (National Electrical Manufacturer's Association) standard, which was developed to provide a uniform criterion for the measurement and reporting of performance parameters for scintillation cameras, and by which a manufacturer may specify his device. The purpose of this paper is to familiarize the nuclear medicine practitioner with the standard, the measurement methods, the reasons for them, and the meaning of the reported values.**

**J Nucl Med 22: 72-77, 1981**

The performance of scintillation cameras can be measured using a variety of tests and procedures that depend on the purpose of the measurement and the test equipment available. Most performance measurements are made for one of three reasons: (a) by the manufacturer to test and specify the equipment he sells, (b) by the customer to test new equipment against the manufacturer's claims, and (c) by the user as part of a periodic quality-control program. For each category the requirements are quite different: for example, in the case of quality-control testing it is important that the test be easily performed and that it test those performance parameters that are likely to change. On the other hand, manufacturer's specifications must be accurate, reproducible, and quantitative to allow intercomparisons.

This paper describes the NEMA performance measurement standard for scintillation cameras, which was developed by the Standards, Technical and Regulatory Committee of the Nuclear Section of the National Electrical Manufacturer's Association (1). The purpose of this standard is to provide uniform criteria for the measurement and reporting of the scintillation-camera

performance parameters by which a manufacturer may specify his device. The standard describes measurements that are sufficiently precise to allow intercomparison of devices from different manufacturers. A customer with adequate test instruments may check his camera against some or all of the specifications, or may ask an independent organization to do so. However, a complete and accurate characterization of the imaging device was the primary objective of this standard, which occasionally dictated the choice of tests not readily repeated elsewhere. We hope that there will soon be computer programs that will allow most of these measurements to be duplicated using computer systems that are in widespread use in nuclear medicine facilities.

Although the NEMA performance measurement standard (1) covers both single- and multiple-crystal scintillation cameras, the present publication describes only the section applicable to single-crystal cameras, and many details are omitted here. Before attempting to duplicate any of the measurements, the reader should refer to the original for a complete description.

The NEMA standard establishes techniques for the specification of the following scintillation-camera parameters: (a) intrinsic spatial resolution, (b) intrinsic energy resolution, (c) flood-field uniformity, (d) spatial linearity, (e) count-rate performance, (f) multiple-window spatial registration, (g) system spatial resolution, and (h) system sensitivity. For each measured param-

\* Present address: Department of Radiology, Hospital of the University of Pennsylvania, Philadelphia, PA.

Received May 21, 1980; revision accepted Sept. 19, 1980.

For reprints contact: Gerd Muehlelehner, PhD, Dept. of Radiology, Hospital of the University of Pennsylvania, Philadelphia, PA 19104.

ter, the manufacturers will specify the "worst-case" number, except in the case of class standards, which will be identified below. Establishing a "worst-case" specification implies that the measurement be performed on a large number of systems and that the performance of new devices be monitored to ensure that the specification is met. Certain time-consuming or less important parameters were therefore declared as class standards, and for these only "typical" values will be reported by the manufacturers.

All of the described tests are performed under conditions typical for static imaging with a 20% energy-window width (except for the measurement of energy resolution) and at count rates varying from less than 10 K cps for spatial resolution and linearity measurements to 30 K cps for uniformity measurements. Below the specified count rates, performance is typically invariant; performance at higher count rates is measured separately to allow an assessment of deterioration of performance with count rate.

INTRINSIC SPATIAL RESOLUTION

Intrinsic spatial resolution shall be measured in both the X and Y directions and expressed as full width at half maximum (FWHM) and full width at tenth maximum (FWTM) of the line spread function. For this and other measurements, two diameters are defined: (a) the useful field of view (UFOV), which is the collimator's field diameter; and (b) the central field of view (CFOV), which is 75% of the diameter of the UFOV. For many clinical applications, the CFOV may be more repre-

sentative of the area occupied by the organ to be imaged; the UFOV measurements will generally be worse due to edge effects.

Line spread functions are measured using a lead mask as close as possible to the crystal and covering the entire field of view. The dimensions of the mask are shown in Fig. 1. A point source of Tc-99m is located at a distance of at least five times the useful field of view in order to avoid magnification of the slit pattern and reduction of sensitivity for slits far from the center. The slit separation of 30 mm appeared adequate for present-day cameras with spatial resolution in the vicinity of 5 mm FWHM without significant overlap between adjacent line spread functions. The choice of a 1-mm slit width was a deliberate trade-off between sensitivity (counting time) and accuracy of the FWHM measurement; the use of a 1-mm slit will lead to a less than 10% overestimation of FWHM for values above 3 mm (2).

The data are digitized with a digitization resolution of not more than 0.1 FWHM perpendicular to the slits, and  $\leq 30$  mm parallel to the slits. The slits, which extend over the full field of view, are thus divided into short, 30-mm line segments, and the profiles at right angles to the slits represent measured line spread functions averaged over 30 mm. Thus many values of resolution over the face of the camera are obtained in one measurement. For a camera with a diameter of 400 mm and a resolution of 4 mm FWHM, approximately 1000 channels are needed perpendicular to the slits to keep the measurement error below 2%. The use of 256 channels will lead to a systematic error of  $\sim 5\%$  in the calculated values (2). The data can of course be taken with a one-parameter

RESOLUTION AND LINEARITY PHANTOM

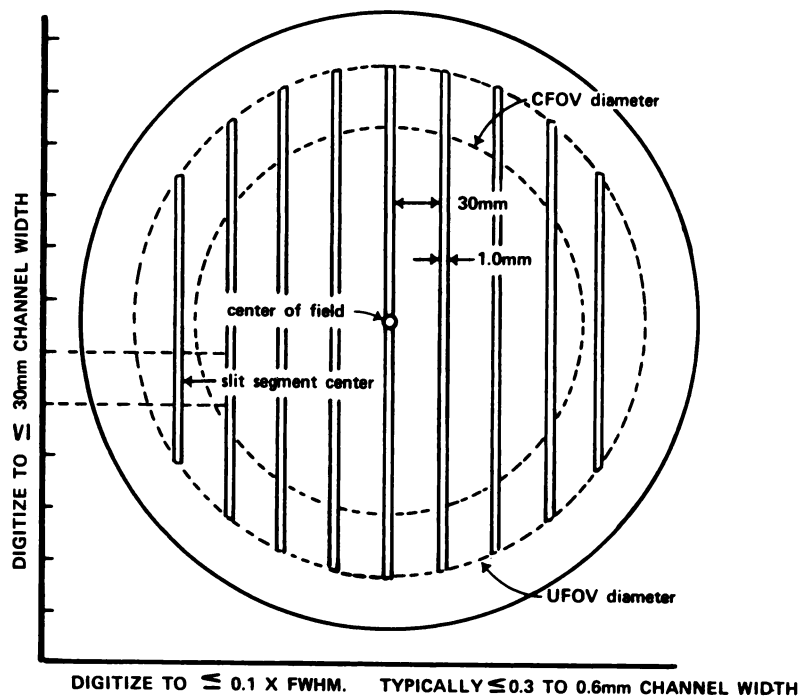


FIG. 1. Outline of lead mask for measurements of intrinsic resolution and linearity. Thickness of mask is 3 mm.

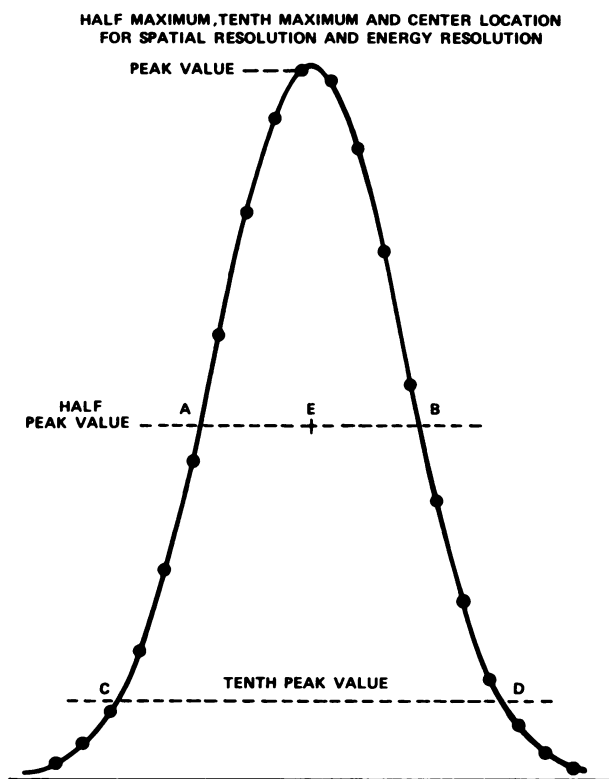


FIG. 2. Sketch illustrating method used to calculate full width at half maximum (FWHM) and full width at tenth maximum (FWTM).

multichannel analyzer and a second lead mask to define successive 30-mm segments on the camera's field of view.

The FWHM and FWTM values are calculated in the following manner (see Fig. 2). The counts registered in the peak channel are divided by two (or ten) to find the half-maximum (or tenth-maximum) value. Since this value is likely to fall between measured values on both sides of the peak, linear interpolation from the nearest two neighboring values is used to find the fractional channel locations on both sides of the peak corresponding to the half- (or tenth-) maximum. The difference between these interpolated, fractional channels is the full width, and since the units are channels, this value must be converted to millimeters. The location of the peak is determined as the average of the interpolated half-height channel values calculated for each side of the peak. Where possible, the separation between the two adjoining peaks will be averaged to determine the millimeters/channel calibration for each peak. Since a separate calibration value is used for each FWHM and FWTM value, possible slight differences in X and Y gain and varying magnification over the field of view are taken into account. The calculated values are not corrected for background or slit width, and all values for the X and Y axes are averaged. For a peak count of 1,000 in each line spread measurement, individual measurements of FWHM and FWTM will show an appreciable error,

but the average value for 50 to 100 measurements will achieve increased precision.

In our experience this technique gives results that are reproducible to better than 0.1 mm. It completely characterizes the resolution of the camera over the field of view and (given the mask and data analysis system) can be performed in a short time. Validation of the results is possible with a 1024-channel analyzer, but requires more data-collection time. Most systematic errors have been eliminated, the most significant remaining error being due to the finite slit width, as discussed above. This error, however, does not invalidate comparative results, since it gives a consistent overestimation.

#### INTRINSIC ENERGY RESOLUTION

Energy resolution shall be measured using a Tc-99m point source located at a distance of at least five times the useful field of view, with no collimator or scattering material interposed between source and detector. It is expressed as the ratio (or percentage) of photopeak FWHM in keV to photopeak energy in keV. The full width at half maximum and location of the peak are calculated using the technique described in the above section on intrinsic spatial resolution. Due to non-linearities of NaI(Tl) and possible offsets in the circuitry, it is important to calibrate the spectrum in keV by using a Co-57 source (energy 122.1 keV).

#### INTRINSIC FLOOD-FIELD UNIFORMITY

Any quantitative description of flood uniformity should be related to the visual judgment of flood quality—i.e., it should show a high degree of correlation with the opinion of a number of observers who are asked to rank flood images according to subjective quality. In general, observers will find a slow change in flood intensity much less objectionable than changes that are similar in size to lesions and, therefore, can interfere with a diagnosis. Sudden changes in flood intensity are visually observable even if they are only a few percent, whereas gradual changes of even 20% are hardly discernible. While a number of quantitative measures of uniformity have been proposed (3,4), these have not been correlated to observer ranking. Before accepting any particular measure of flood uniformity as a standard, a study was undertaken (Moyer RA, Stoub EW, unpublished data) to correlate various numerical techniques with observer ranking using more than 100 flood images and five observers. The numerical techniques included deviation from a bowl-shaped function, standard deviation, and integral and differential measures of uniformity (see below) calculated for flood data from the UFOV and CFOV area. None of the quantitative measures showed a correlation coefficient exceeding 0.5—particularly with the flood data from the UFOV—whereas observers showed a correlation of

better than 0.8 among each other. It must be concluded that the eye is still the best qualitative judge of uniformity and quantitative measures proposed so far give only a rough indication of flood quality.

With these reservations in mind, two measures of flood-field uniformity were chosen: (a) integral uniformity as a measure of maximum deviation, and (b) differential uniformity as a measure of maximum rate of change over a short distance. In addition, variations of point-source sensitivity are measured.

Floods are accumulated with a point source of Tc-99m located at a distance of at least five times the useful field of view and with a minimum of 4000 counts per image element in a 64 X 64 matrix at the center of the image. In spite of an accumulation of ~12 million counts, the data must be smoothed once with a nine-point filter function having the following weightings:

$$\begin{matrix} 1 & 2 & 1 \\ 2 & 4 & 2 \\ 1 & 2 & 1 \end{matrix}$$

Without smoothing, several matrix elements are likely to be found deviating more than three standard deviations from the mean, or roughly ±5%. Since the integral uniformity will be comparable to 5% (at least for systems with uniformity-correction devices) the smoothing is required to reduce the random variations.

Integral uniformity is determined by searching for the maximum and minimum values within the area of interest (CFOV or UFOV) and evaluating the expression

$$\text{Integral uniformity} = \pm 100 \frac{\text{Max} - \text{Min}}{\text{Max} + \text{Min}}$$

Differential uniformity is a measurement of the worst-case rate of change of the flood field over a limited distance. The flood is treated as a number of rows and columns (slices). Each slice is processed by examining five pixels from the first pixel within the field of view and recording the maximum difference. The start pixel is moved forward one pixel and the next five pixels are examined: This process is continued for all pixels in each slice and the largest positive (+Max) and negative (-Max) deviation for all slices is determined. Differential uniformity is then derived as

$$\text{Differential uniformity} = \pm 100 \frac{(+\text{Max}) - (-\text{Max})}{(+\text{Max}) + (-\text{Max})}$$

The range of search for differential uniformity corresponds approximately to the photomultiplier radius in a 37-tube camera. Many flood-field defects occur with a frequency of one cycle per tube diameter and are thus detected with this definition of differential uniformity.

Flood-field nonuniformities can result from (a) small spatial distortions and (b) variations in point-source sensitivity (5, 6). Particularly for quantitation it is im-

portant to separate the two effects and measure the variations in point-source sensitivity. As a class standard, point-source sensitivity shall be measured with a collimated small source of Tc-99m at each point of a matrix centered in the UFOV with 3 cm between points on each axis. The number of counts registered during a fixed time interval are recorded. The time interval must be chosen long enough to assure accumulation of more than 100,000 counts for each point in the matrix. After decay correction, sensitivity variation is obtained by evaluating the expression

$$\text{Sensitivity variation} = \pm 100 \frac{\text{Max} - \text{Min}}{\text{Max} + \text{Min}}$$

#### INTRINSIC SPATIAL LINEARITY

As in the case of flood uniformity, linearity must be defined through absolute linearity, which measures the maximum deviation from an ideal rectangular grid, and through differential linearity, which measures short-range deviations from a straight line. For both measures of linearity, the same data can be used as for the resolution measurement, since these are derived from short, parallel, equal-spaced line segments in both X and Y direction.

Absolute linearity is determined by establishing an ideal grid from the measured data and determining the maximum displacement from this grid. It is quoted in millimeters. The ideal grid is established by using the average spacing of peaks within the field of view. Differential linearity is given by the standard deviation, in millimeters, for adjacent peak separations between all peaks in the specified field of view. Since each line segment is 30 mm long, very abrupt nonlinearities are averaged out; instead, this measure of differential linearity is sensitive to distortions between photomultiplier tubes. The measurement of smaller distortions at high spatial frequencies is possible (6), but requires much higher accuracy and better statistical data.

#### INTRINSIC COUNT-RATE PERFORMANCE

Five parameters are used to characterize the count-rate performance of scintillation cameras: (a) input count rate for a 20% count loss, (b) maximum count rate, (c) the typical incident-as-opposed-to-observed count-rate curve, (d) intrinsic spatial resolution at 75,000 cps (observed), and (e) intrinsic flood-field uniformity at 75,000 cps (observed). The first two parameters are "worst case" specifications; the latter three either require large amounts of activity or are of secondary importance; they are therefore typical values, i.e., they are quoted as class standards.

The rate for 20% count loss will be calculated on the assumption that the camera behaves as a purely para-

lyzable system below the 20%-loss rate, and thus will follow the formula:

$$R_o = R e^{-R\tau}$$

where  $R$  is the input rate and  $R_o$  is the observed rate. The deadtime,  $\tau$ , shall be determined by a modified two-source measurement (7) and calculated according to the formula:

$$\tau = \frac{R_{12}}{(R_1 + R_2)^2} \ln \frac{(R_1 + R_2)}{R_{12}}$$

where  $R_1$ ,  $R_2$ , and  $R_{12}$  will be described below. The count rate for 20% count loss ( $R_{-20}$ ) will be calculated from the formula:

$$R_{-20} = \frac{1}{\tau} \ln \left( \frac{10}{8} \right) = \frac{0.2231}{\tau}$$

The data are acquired by masking the camera crystal to the UFOV and suspending one source near its axis at some distance, greater than one meter, that will provide the desired count rate ( $R_1$ ). A second source with activity within  $\pm 10\%$  of the first is added in such a fashion that neither source obscures the other's view of the crystal, and the combined rate ( $R_{12}$ ) is recorded. After removing the first source,  $R_2$  is measured. To compensate for the decay of Tc-99m, the procedure is repeated in reverse order. The count rate with both sources present,  $R_{12}$ , should approximate the anticipated count rate for 20% loss. The above formula does not include the effects of energy-window selection, which reduce the number of counts actually displayed. However, the rate at which 20% of the incoming counts are lost (due to pulse pileup and paralyzable deadtime) is generally not affected by subsequent data loss. Most cameras are not purely paralyzable systems, so this calculation is an approximation only. Furthermore, deadtime may be dominated by slower readout and display devices or by digital circuits for uniformity correction, and therefore depends on the particular configuration.

The maximum count rate is determined by slowly approaching the detector with a source containing  $\sim 2$  mCi Tc-99m and recording the maximum rate. Care must be taken to minimize scatter. This is a comparative value only; it is indicative of counting losses at lower rates and in the presence of scattering material, but the absolute value cannot be achieved in clinical studies.

As a class standard, the data for a typical incident, as opposed to observed count-rate curve, is measured as follows:

As shown in Fig. 3, a small source of Tc-99m in a shielded container is positioned 1.5 m from the face of the detector. The source intensity is varied by placing a stack of copper absorbers,  $\sim 2.5$  mm thick, over the source. The attenuation of photons by each copper absorber must be measured previously. The number of absorber plates to produce a background-corrected count

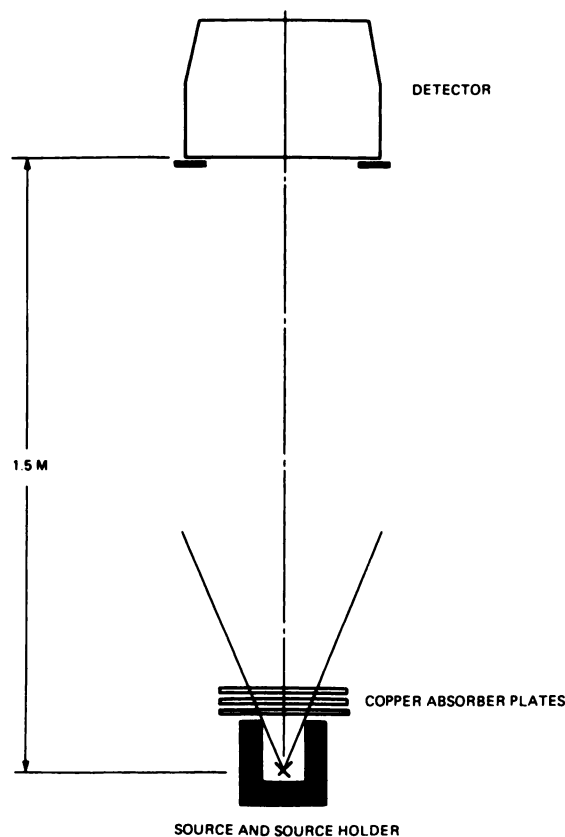


FIG. 3. Geometry used to measure data for count-rate curve.

rate no greater than 2,500 cps is determined. From this count rate, knowing the calibration of each absorber and the decay rate of the source, various known incident count rates can be obtained by sequential removal of absorber plates. This technique provides a method for obtaining a complete count-rate curve without relying on any particular model; it has been found to give essentially the same results as the decaying-source method and it is less time-consuming.

In order to determine the extent to which resolution and uniformity are degraded at high count rates, such as might be encountered in first-pass cardiac studies, the procedures described above to measure intrinsic spatial resolution and intrinsic flood-field uniformity are repeated at observed count rates of 75,000 cps.

#### MULTIPLE-WINDOW SPATIAL REGISTRATION

In studies using multiple energy windows, e.g., with Ga-67, it is important that events collected through two, or all three, windows should be displayed in the identical location in order to avoid loss of resolution. The spatial registration of images from each of the camera's energy windows is measured using a Ga-67 source collimated through a hole 3 mm in diameter and at least 6 mm in length. This source is placed sequentially on the +X, -X, +Y, and -Y axes, at a distance from the center of the UFOV circle equal to 75% of its radius. An image is

accumulated at each position and through each energy window independently; and the source location is determined, from which the maximum registration error can be calculated.

#### SYSTEM SPATIAL RESOLUTION

While intrinsic spatial resolution is a convenient parameter for comparison of systems, the performance of cameras in clinical situations is better characterized by system resolution. This, however, is a function of the particular collimator used, and the large variety of collimators available makes system comparisons more difficult. Information on system resolution as a function of distance and system sensitivity is necessary in selecting the appropriate combination for a particular clinical study.

System resolution (both FWHM and FWTM) is measured with and without scattering material in both X and Y directions for a specified collimator. For this measurement, a line source with an inside diameter less than 1 mm is filled with Tc-99m and placed at various distances from the collimator, in 50-mm increments and including a distance of 100 mm. For the measurement with scatter, 100 mm of acrylic plastic, such as Lucite, will be placed between the collimator and the source, and a similar 50 mm sheet of plastic behind the source. A second calibration measurement must be performed with a second line source, placed parallel to the first, 50 mm away from it, and at the same distance from the collimator. The data are collected and analyzed in the same manner as for the measurement of intrinsic resolution; however, at least 10,000 counts must be collected at the peak point of each line spread function to assure accuracy in the calculated values.

Due to the variety of collimators available, a complete set of data, even from a single manufacturer, demands a large number of individual measurements. System resolution is therefore quoted as a class standard; in addition, a new system resolution ( $R_s$ ), due to improvements in intrinsic resolution ( $R_i$ ), can be calculated from the expression

$$R_s = \sqrt{R_c^2 + (R_i/M)^2}$$

where  $R_c$  = collimator resolution and  $M$  = image size/object size, the image magnification factor for converging or diverging collimators.

#### SYSTEM SENSITIVITY

System sensitivity is measured for each collimator in units of cpm/ $\mu$ Ci using a 20% energy window. In order to avoid attenuation, the activity is dispersed into a shallow solution ( $\sim 3$  mm deep) in a 100-mm diameter Petri dish. The activity placed in the dish must be determined accurately by measuring a syringe both before and after discharging the activity from it. The dish is

placed near the center of the collimator's field of view, 100 mm from the face of the collimator, and the counts per minute are recorded.

#### DISCUSSION

The NEMA tests to characterize the imaging characteristics of scintillation cameras are technically complex and require some expertise to understand or duplicate. Furthermore, the final list of parameters to be reported exceeds 50 even if only four collimators are included. On the other hand, many potentially valuable parameters have been omitted, such as resolution and uniformity for other nuclides (Tl-201 and Ga-67, for example), uniformity as a function of energy window width, deadtime in the presence of scatter, modulation transfer function, and others. Thus it may be argued that the standard is either too complex or not detailed enough, yet it represents the basis for a uniformity of published specifications. It will doubtless evolve and be further refined.

The reason for establishing the standard was to develop a "common language" for manufacturers and customers alike; general acceptance of these standards will help the customer in selecting devices and help the manufacturer in communicating with hospital physicists, physicians, and technologists.

#### ACKNOWLEDGMENTS

The NEMA standard was developed under the expert guidance of Paul F. Peters, with valuable help from all members of the NEMA Standards, Technical and Regulatory Committee, Nuclear Section, and with helpful input from many physicians and physicists active in nuclear medicine. All this assistance is gratefully acknowledged. We particularly thank R. A. Moyer, D. Persyk, S. Webe, and H. Wilson for their contributions during various phases of the development of the standard.

#### REFERENCES

- Standards Publ. No. NU1-1980. Performance measurements of scintillation cameras. National Electrical Manufacturers Association, Washington, DC, 1980
- SCHARDT MA, RITTER KA, COLSHER JG: Systematic errors in digital resolution measurements of gamma cameras. *Med Phys* 7:415, 1980 (abst)
- KEYES JW, GAZELLA GR, STRANGE DR: Image analysis by on-line minicomputer for improved camera quality control. *J Nucl Med* 13:525-527, 1972
- HASMAN A, GROOTHEDDE RT: Gamma-camera uniformity as a function of energy and count-rate. *Br J Radiol* 49:718-722, 1976
- TODD-POKROPEK AE, ERBSMAN F, SOUSSALINE F: The nonuniformity of imaging devices and its impact in quantitative studies. In *Medical Radionuclide Imaging*. vol 1. Vienna, IAEA, 1977, pp 67-84
- MUEHLEHNER G, COLSHER JG, STOUB EW: Correction for field nonuniformity in scintillation cameras through removal of spatial distortion. *J Nucl Med* 21:771-776, 1980
- ADAMS R, HINE GJ, ZIMMERMAN CD: Deadtime measurements in scintillation cameras under scatter conditions simulating quantitative nuclear cardiology. *J Nucl Med* 19:538-544, 1978